eNeuro

Research Article: New Research | Integrative Systems

Mouse adrenal macrophages are associated with pre- and post-synaptic neuronal elements and respond to multiple neuromodulators

https://doi.org/10.1523/ENEURO.0153-24.2025

Received: 3 April 2024
Revised: 21 December 2024
Accepted: 13 January 2025

MOUSE ADRENAL MACROPHAGES ARE ASSOCIATED WITH PRE- AND POST-SYNAPTIC NEURONAL ELEMENTS AND RESPOND TO MULTIPLE NEUROMODULATORS

Abbreviated title: Immune cells and the adrenal medulla

Author: Matthew D. Whim

Department of Cell Biology & Anatomy, LSU Health Sciences Center, New Orleans, LA 70112, USA.

Author contributions: MDW designed research, performed research, analyzed data and wrote the paper

Address for correspondence:

Matthew D. Whim,

Department of Cell Biology and Anatomy,

LSU Health Sciences Center,

Clinical Sciences Research Building, CSRB 601B

2020 Gravier Street, New Orleans, LA 70112, USA

Tel: 504-568-2269

Fax: 504-568-4392

ORCID ID: 0000-0002-8311-1544

E-mail: mwhim@lsuhsc.edu

Tel: 504-568-2269

Fax: 504-568-4392

Figures: 8. Extended Data Figures: 5.

Abstract: 179 words

Significance Statement: 116 words

Introduction: 536 words

Discussion: 1174 words

Acknowledgments: I thank Dr.'s June Liu and Ben Kelly for experimental advice and for critically reading the manuscript.

Conflict of interest: Author reports no conflict of interest

Funding sources: This work was supported by the National Institutes of Health with funding from the National Center for Advancing Translational Sciences (R03TR002929) and the National Institute of Allergy and Infectious Diseases (R21AI178406).

ABSTRACT

The adrenal medulla is packed with chromaffin cells, modified postganglionic sympathetic neurons that secrete the catecholamines, epinephrine and norepinephrine, during the fight-or-flight response. Sometimes overlooked, is a population of immune cells that also resides within the gland but whose distribution and function is not clear. Here I examine the location of CD45+ hematopoietic cells in the mouse adrenal medulla and show the majority are F4/80+/Lyz2+ macrophages. These cells are present from early post-natal development and widely distributed. Anatomically they are associated with chromaffin cells, found aligned alongside synapsin-ir neuronal varicosities and juxtaposed to CD31-ir blood vessels. Using Lyz2cre-GCaMP6f mice to quantify calcium signaling in macrophages revealed these cells respond directly and indirectly to a wide variety of neuromodulators, including pre- and post-ganglionic transmitters and systemic hormones. Purinergic agonists, histamine, acetylcholine and bradykinin rapidly and reversibly increased intracellular calcium. These results are consistent with a substantial resident population of innate immune cells in the adrenal medulla. Their close association with chromaffin cells and the preganglionic input suggests they may regulate sympatho-adrenal activity and thus the strength of the fight-or-flight response.

SIGNIFICANCE STATEMENT

It is widely recognized that the nervous and immune systems can functionally communicate but many aspects of the underlying cellular mechanisms remain to be clarified. The adrenal medulla contains neuroendocrine chromaffin cells and a diverse population of immune cells whose distribution and function is not well understood. Using immunohistochemistry, I show the medulla contains a large population of macrophages that are closely associated with the pre-ganglionic input and with chromaffin cells. Monitoring calcium levels in macrophages within the mouse adrenal medulla shows these cells can rapidly respond to the application of a wide variety of neuromodulators. Their location and responsiveness suggests these cells could be involved in neuro-immune crosstalk during autonomic activation and the fight-or-flight response.

INTRODUCTION

During the fight-or-flight response, sympathetic activation increases the activity of adrenal chromaffin cells and the release of the catecholamine hormones, epinephrine and norepinephrine into the systemic circulation. For example, in response to hypoglycemia, autonomic activation and subsequent epinephrine release stimulates adipose tissue lipolysis, hepatic glycogenolysis and inhibits pancreatic insulin release (Cryer, 1993; Stanley et al., 2019).

Given the wide-ranging actions of the catecholamines, the activity of the chromaffin cells must be tightly regulated. The increase in chromaffin cell excitability during a stress response is controlled by the activity of sympathetic preganglionic neurons that innervate the adrenal medulla, and which make excitatory, cholinergic synaptic connections onto chromaffin cells. Adrenal denervation or inhibition of cholinergic transmission prevents epinephrine release in response to multiple stressors (Kvetnanský et al., 1996; Lamarche et al., 1992; McKinley et al., 2022; Zhou and Jones, 1993). In addition, paracrine signaling pathways fine-tune chromaffin cell activity. Recent work has shown that an intra-adrenal feedback loop which involves the release of neuropeptide Y from chromaffin cells, is required for sustained epinephrine release. Loss of this pathway likely contributes to HAAF, an activity-dependent impairment of epinephrine release observed in type I diabetes (Ma et al., 2018; Wang et al., 2016).

This suggests that additional signaling pathways that control epinephrine release, beyond the preganglionic input, remain to be identified. Possible candidates involve immune cells located in the adrenal gland. Early work identified macrophages in the rodent adrenal cortex and medulla (Engström et al., 2008; Hume et al., 1984; Sato, 1998; Schober et al., 1998) and macrophages are also present in the human adrenal (González-Hernández et al., 1994; Wang et al., 2023). While the function of these cells is not clear, in vivo injection of LPS results in a dramatic infiltration and reorganization of macrophages and dendritic cells throughout the rodent adrenal (Engström et al., 2008). A recent RNA-seq study demonstrated that the rodent adrenal contains a diverse population of immune cells in addition to macrophages, including T cells, B cells, dendritic cells, monocytes and neutrophils (Dolfi et al., 2022). Systemic macrophage depletion reduces adrenal aldosterone synthesis (Dolfi et al., 2022) and *in vitro*, multiple cytokines including IL-1β and IFN-α can regulate adrenal catecholamine synthesis and release (Douglas and Bunn, 2009; Rosmaninho-Salgado et al., 2009). Finally, several studies have shown that activated macrophages, or macrophage-conditioned medium, can increase epinephrine secretion and modulate voltage-gated calcium channels in chromaffin cells (Currie et al., 2000; Jones et al., 1993; Lujan et al., 1998; Roberts et al., 1996; Roberts and Jones, 1997).

Although these studies are consistent with a role for immune cells in modifying adrenal output, whether these actions are mediated by cells that reside within the adrenal is unclear. This is particularly relevant in the context of the adrenal medulla, given the growing appreciation of crosstalk between the autonomic and immune systems (Klein Wolterink et al., 2022; Pavlov et al., 2018). Using a combination of immunohistochemistry and live cell imaging I now show that the adrenal medulla contains a population of macrophages that are closely associated with chromaffin cells and the pre-ganglionic input. Because these resident innate immune cells can respond to a variety of neuromodulators, this suggests they may be involved in modulating the sympatho-adrenal component of the fight-or-flight response.

MATERIALS AND METHODS

Animals: C57BL/6J wild type mice were bred from a laboratory colony. Lyz2cre mice ((Clausen et al., 1999); JAX #004781), LSL-Salsa6f mice ((Dong et al., 2017); JAX #031968) and NPYcre mice ((Milstein et al., 2015); JAX #027851) were obtained from The Jackson Laboratory. Animals of both sexes were used. All experiments were approved by the institutional animal care and use committee at Louisiana State University Health Sciences Center.

Calcium imaging: to express the GCaMP6f calcium sensor in myeloid cells, Lyz2cre mice were crossed to LSL-Salsa6f mice . The Lyz2cre line is widely used for targeting macrophages but is also expressed in other immune cells including granulocytes (Hume, 2011). Adrenal glands were isolated from male and female Lyz2cre-GCaMP6f-tdTomato mice that were euthanized by decapitation (P22 - P56). Adrenal sections (100 µm) were prepared largely as previously described (Wang et al., 2016). In brief, the glands were embedded in low melting point agarose, the tissue blocks were trimmed, then mounted on a Leica VT100 vibratome. Sections were cut in ice-cold ACSF (artificial cerebral spinal fluid; 125 mM NaCl, 3 mM KCl, 2 mM $CaCl_2$, 1 mM $MgCl_2$, 25 mM $NaHCO_3$, 1.25 mM NaH_2PO_4, 5.5 mM glucose, pH 7.4) that was bubbled with 95% O_2 / 5% CO_2. The sections were subsequently transferred to the same solution maintained at room temperature (22-24 °C). To monitor calcium activity, a single adrenal slice was transferred to an imaging chamber on the stage of a Nikon TE2000U inverted microscope. The chamber (volume ~ 600 µl) was continually superfused at ~ 3 ml / minute with extracellular solution (135 mM NaCl, 3 mM KCl, 2 mM $CaCl_2$, 1 mM $MgCl_2$, 10 mM HEPES, 5.5 mM glucose, pH 7.4) at room temperature. In some experiments (Fig 7D), the extracellular solution contained 0 mM $CaCl_2$ and 2 mM EGTA. Slices were viewed with a 20x objective and illuminated using a DG-4 xenon light source (Sutter Instruments). A region of the medulla containing macrophages was identified by RFP (red fluorescent protein) expression in Lyz2cre-GCaMP6f-tdTomato mice (excitation 530 – 550 nm / emission 590 – 650 nm) and positioned in the center of the field of view. The GCaMP6f signal (excitation 460 – 500 / emission 510 – 560 nm) was collected (500 ms exposure time) every 5 sec using NIS-Elements (Nikon Imaging Software). To quantify changes in $[Ca^{2+}]_i$, ROI's were drawn around 10-15 individual cells identified in the RFP channel and the mean fluorescence change was then quantified in the GFP channel. This approach avoided inadvertently biasing the data collection to cells that showed the largest change in calcium levels. Fiji/ImageJ (Schindelin et al., 2012), Clampfit10 (Molecular Devices), Origin2019b (OriginLab) and Excel were used for data analysis. In each figure the number of biological replicates (n = number of mice) is noted. Changes in GCaMP6f signal in response to agonist application were performed on raw data and calculated as Ft-F0 (fluorescence at time t - fluorescence immediately before agonist application). For example recordings (Figures 6, 7), slow changes in baseline signal over the course of an experiment were removed using Clampfit.

Additional tissue and cell type isolation from Lyz2cre-GCaMP6f-tdTomato mice: (i) *adrenal cells* (both cortex and medulla) were dissociated using enzymatic digestion as previously described for chromaffin cells (Whim, 2006). Dissociated cells were plated on poly-d-lysine coated coverslips in DMEM / 10% FCS. After allowing 1 hr for attachment, the cells were subsequently used within 6 hrs of isolation. (ii) *peritoneal macrophages* were collected from euthanized mice by peritoneal lavage with 3 ml DMEM / 10% FCS. After centrifugation (1,000 rpm for 3.5 minutes), the pellet was resuspended in DMEM / 10% FCS and cells were plated on uncoated coverslips and used within 6 hrs. Staining indicated most cells in these cultures were F4/80-ir (83 ± 3 %, mean ± SEM, 76 cells from n = 3 mice). (iii) *lung tissue slices* were prepared using the same approach as described for the adrenal gland. Small pieces of pulmonary tissue were dissected from the base of the right lung of euthanized mice and embedded in low melting point

agarose. After isolation, tissue sections (100 µm) were maintained at room temperature in ACSF bubbled with 95% O_2 / 5% CO_2. Because both pulmonary macrophages and alveolar type 2 (epithelial) cells express lysozyme 2 (and thus GCaMP6f), macrophages were identified as those cells which showed an increase in $[Ca^{2+}]_i$, in response to 100 µM nicotinic acid, a HCAR2 (hydroxycarboxylic acid receptor 2) agonist. The LungMAP RNA-seq dataset (lungmap.net) indicates HCAR2 is strongly expressed by alveolar macrophages but not alveolar type 2 cells.

Immunohistochemistry: adrenal glands were isolated from male and female C57BL/6J wild type and Lyz2cre-GCaMP6f-tdTomato mice that were euthanized by decapitation. Glands were fixed in 4% paraformaldehyde for 1 hr at 4 °C, then washed with PBS and transferred to PBS / 30% sucrose for 24 hr at 4 °C. Glands were snap frozen in 2-methylbutane on dry ice, embedded in OCT (Optimal Cutting Temperature compound) and 30 µm cryosections were prepared and stored in cryoprotectant (Watson et al., 1986) at -20 °C until used. For staining, sections were removed from cryoprotectant, washed with PBS (containing 0.05% Triton X100), then incubated sequentially in 3% H_2O_2 and 2 mg / ml sodium borohydride (each for 20 minutes) at room temperature. Sections were incubated shaking overnight at 4 °C or at room temperature in primary antibody (diluted in PBS / 1% IgG-free BSA / 0.3% Triton). Next day, the sections were washed with PBS. For TSA (Tyramide Signal Amplification) staining, sections were incubated in HRP-coupled secondary antibodies (1:250 diluted in PBS / 1% IgG-free BSA / 0.05% Triton) for 30 minutes at room temperature. After washing, the sections were incubated in 1:50 TSA-FITC or TSA-TMR reagent following the manufacturer's instructions (PerkinElmer), then washed and mounted in Vectashield (VectorLabs). For regular indirect immunofluorescence, after overnight incubation in primary antibody, the sections were washed, incubated for 90 mins at room temperature in 1:100 fluorescently labelled secondary antibody, then washed in PBS and mounted in Vectashield. Before mounting, all sections were incubated in DAPI for 15 minutes at room temperature (1 µg / ml in PBS / 0.05% Triton) to stain cell nuclei. Primary antibodies were rat anti-CD45 (1:10,000, BioLegend BL103101, RRID AB_312966); rat anti-F4/80 (1:5,000, BioLegend BL123101, RRID AB_893504); rat anti-CD68 (1:20,000, BioLegend BL137001, RRID AB_ 2044003); rat anti-CD301 (1:5,000, Abd Serotec MCA2392, RRID AB_872014); rat anti-CD115 (1:5,000 BioLegend BL135501, RRID AB_1937292); rat anti-MHC II (1:10,000, BioLegend BL107601, RRID AB_313316); rat anti-Iba1 (1:2,000, Cell Signaling Technology CST17198, RRID AB_2820254); rabbit anti-RFP (1:1,000, Rockland 600-401-379, RRID AB_2209751); chicken anti-RFP (1:20,000, Rockland 600-901-379, RRID AB_10704808); rabbit anti-tyrosine hydroxylase (1:2,000, Cell Signaling Technology CST2792, RRID AB_2303165); guinea pig anti-PNMT (1:200, Acris EDU7001, RRID AB_1006533); rabbit anti-NPY (1:10,000, Peninsula T4070, RRID AB_518504); rabbit anti-GFAP (1:200, Dako Z0334, RRID AB_10013382); rabbit anti-MAP2 (1:500, Millipore AB5622, RRID AB_91939); rat anti-CD31 (1:200,000, BioLegend BL102501, RRID AB_312908); rabbit anti-acetylated tubulin (1:2,000 Cell Signaling Technology CST5335, RRID AB_10544694); rabbit anti-synapsin (1:500, Millipore AB1543, RRID AB_2200400). Secondary antibodies (all from Jackson ImmunoResearch) were donkey anti-rat HRP (1:250); donkey anti-chicken HRP (1:1,000); donkey anti-rabbit Cy3 (1:100); donkey anti-rabbit Alexa 488 (1:100) and donkey anti-guinea pig FITC (1:100). Images were obtained with a Nikon TE2000U inverted microscope with 10x and 40x objectives and a DG-4 xenon light source. When using the 40x objective, z-stacks (11 images collected in the z-plane with a 1.2 µm step size) were deconvolved using NIS-Elements (Nikon) software (using blind 3D deconvolution with a theoretical point spread function and no background subtraction). This was adopted because even in 30 µm cryosections, some out-of-

focus fluorescence was present (medulla macrophages are thin cells with wandering processes that do not lie in the horizontal plane). However, all quantitative measurements were made on data obtained with the 10x objective and these were not deconvolved.

To quantify the degree of co-localization (Fig 6A) a threshold criterion was used to identify stained cells. This was met by cells whose mean fluorescence intensity exceeded the "background + 2 x SD" as previously described (Glynn and McAllister, 2006). In brief, background was first quantified individually for each stained section by placing ROI's around 10 clearly stained cells in each fluorescence channel. Each ROI was then displaced adjacent to the stained cell (avoiding cell-free areas such as medulla sinusoids) and the mean intensity + (2 x SD) was calculated. Any cell in the medulla whose level of fluorescence exceeded this value was then scored as positive. The advantage of this method is that background fluorescence is measured on a slide-by-slide basis. However, other approaches (for example staining wild type mice with RFP primary and secondary antibodies) confirmed that the background was low (Extended Data Fig 6-1A-D). Figures were assembled using Fiji and Inkscape.

Statistical tests: comparisons between groups that contained normally distributed data (assessed using the Shapiro-Wilk test) were made using analysis of variance (Tukey post hoc). The Kruskal-Wallis ANOVA (Dunn's post hoc) was used for non-normal data. Origin2019b and Excel were used for analysis. All values are mean ± standard error of the mean (SEM) and $P < 0.05$ was considered significant. Table 1 lists the tests used in this study.

Table 1

Data structure	Type of test	Power
Fig 5G	Non-normal; Kruskal-Wallis ANOVA	NS
Fig 6B	Normal distrib; One way ANOVA	0.05
Fig 6C	Normal distrib; One way ANOVA	0.01-0.001
Fig 7C (pyrillamine)	Normal distrib; One way ANOVA	0.5-0.01
Fig 7C (cimetidine)	Non-normal; Kruskal-Wallis ANOVA	NS
Fig 7D (rapid)	Normal distrib; One way ANOVA	0.5
Fig 7D (slow)	Non-normal; Kruskal-Wallis ANOVA	NS

RESULTS

Macrophages are widely distributed throughout the adrenal medulla

To visualize immune cells in the adrenal, cryosections were stained for expression of CD45, which labels all hematopoietic cells. CD45-ir cells were present throughout all adrenal zones (Fig 1A). Within the medulla, the majority of CD45-ir cells had numerous fine processes (Fig 1B) although occasional spherical cells were also found (Fig 1C). Consistent with a significant adrenal population of macrophages, many F4/80-ir cells were present, including within the medulla (Fig 2A,B). The X-zone, a cortical zone that degenerates postnatally in mice (Hershkovitz et al., 2007), was strongly immunoreactive (Fig 2A).

Macrophages are molecularly and functionally plastic cells. Historically they have been separated into M1 and M2 populations (classically activated and proinflammatory versus alternatively activated and anti-inflammatory, respectively). It is now recognized that

macrophage state exists on a continuum with their physiology being determined by developmental origin, environmental context and tissue location (Katkar and Ghosh, 2023). I next selected a variety of commonly used macrophage markers to examine the distribution of these cells with particular attention to those located in the medulla. Staining for CD68 (a lysosomal associated membrane protein) and CD301 (Clec10A, C-type lectin domain family 10A) labelled cells within the cortex but only a modest number of cells in the medulla (Fig 2C,D). Immunoreactivity for the CSF1 receptor (CD115) which is differentially expressed in tissue macrophages, labelled very few cells in the medulla (Fig 2E). MHC II (major histocompatibility II), a marker of antigen-presenting cells, showed labelling throughout the cortex with lower staining in the medulla (Fig 2F). In contrast, Iba1-ir (ionized calcium binding adaptor 1) which is highly expressed by microglia, showed intense staining in all adrenal zones (Fig 2G). Staining adrenal sections for both F4/80 and Iba1 showed that the majority of cells were co-labelled (Extended Data Fig 2-1) indicating that they identified the same population of macrophages. Finally, using a Lyz2cre transgenic line which is widely used to identify macrophages (and monocytes), revealed that many Lyz2-expressing cells were present in the medulla (Fig 2H). Thus, there is an extensive population of tissue resident macrophages in the rodent adrenal medulla, as previously reported (Dolfi et al., 2022; Engström et al., 2008; Hume et al., 1984; Sato, 1998; Schober et al., 1998). Two recent RNAseq studies have profiled mouse adrenal cells and identified three (Bedoya-Reina et al., 2021) or four (Dolfi et al., 2022) populations of adrenal macrophages. Comparing the staining profile in Fig 2 with transcript expression in these studies indicated it was not possible to categorically assign medulla macrophages. For example, Iba1 was highly expressed in all three macrophage populations in Bedoya-Reina et al (Bedoya-Reina et al., 2021); restricted to cluster #2 in Dolfi et al (Dolfi et al., 2022) and immunohistochemically labelled cortical and medulla macrophages (Fig 2G).

Macrophages are associated with pre- and post-ganglionic cells in the adrenal medulla

To determine whether the medulla macrophages are present in discrete anatomical niches, the co-localization of F4/80-ir and markers of other medulla cell types was examined. The rationale for selecting the F4/80 antibody was that the F4/80 (Adgre1) antigen is the most widely used marker of tissue-resident macrophages and the Adgre1 transcript is reportedly present in all adrenal macrophages (Dolfi et al., 2022). F4/80-ir cells were closely associated with chromaffin cells that were visualized with TH-ir (Fig 3A,B). Macrophages were juxtaposed to both PNMT positive and negative cells indicating that the immune cells were associated with both epinephrine- and norepinephrine-secreting chromaffin cells (Fig 3C,D). NPY is a peptide co-transmitter that is expressed by all mouse chromaffin cells (Wang et al., 2013), and F4/80-ir macrophages were apposed to NPY-ir cells as expected (Fig 3E,F). GFAP-ir, a marker of satellite glial cells (Avraham et al., 2020; Hanani and Spray, 2020), was restricted to the medulla and the adrenal capsule. Co-staining with F4/80 and GFAP showed macrophages and glial cells were often juxtaposed (Fig 3G,H). Finally, labeling with CD31 to visualize the endothelial cells that line blood vessels, revealed that some Lyz2-expressing macrophages also extended processes that appeared to contact blood vessels within the medulla (Fig 3I,J).

Recent studies have identified a population of macrophages that can functionally interact with peripheral autonomic nerves (Pirzgalska et al., 2017; Ural et al., 2020; Wolf et al., 2017). To determine whether macrophages are associated with the preganglionic input to the adrenal, cryosections were stained for acetylated tubulin which is enriched in axons (Cambray-Deakin

and Burgoyne, 1987). F4/80-ir cells were in close contact with acTub-ir processes and often aligned alongside acTub-ir structures (Fig 4A,B). To confirm the association of macrophages and neuronal processes, I next stained for synapsin, a synaptic vesicle protein. Many F4/80-ir cells were juxtaposed to synapsin-ir puncta (Fig 4C,D). The adrenal also receives vagal afferent and efferent input (Coupland et al., 1989), sensory innervation from dorsal root ganglia (Mohamed et al., 1988; Zhou et al., 1991) and limited post-ganglionic input (Kesse et al., 1988). However, the acTub- and synapsin-ir structures likely reflect the dense innervation of the medulla by cholinergic sympathetic preganglionic neurons (Gautron et al., 2013; Kesse et al., 1988). Examination of z-stacks confirmed the close association between macrophages and chromaffin cells, glial cells, endothelial cells and axons (Extended Data Fig 3-1).

Finally, to determine whether adrenal macrophages are present throughout post-natal development I examined the presence of F4/80-ir cells in neonatal (P1) mice and at P7, P25 and P50. Macrophages were evident in the medulla at all time points (Fig 5A-D) and in both sexes (Fig 5C-F). Although there was a tendency for fewer F4/80-ir cells at P50, this was not statistically significant (Fig 5G). There was also no difference in the number of Iba1-ir cells in the medulla of female and male at P50 (6.05 ± 0.53 *vs* 6.7 ± 0.84, mean # / 0.01 mm^2 ± SD, n = 3 mice, P = 0.31).

In sum, these findings indicate the presence of a large population of tissue resident macrophages in the mouse adrenal medulla. Although these cells do not appear to be restricted to particular regions within the medulla, they are anatomically close to both pre- and post-synaptic neuronal components (preganglionic neurons and chromaffin cells, respectively). One implication of this physical arrangement is the existence of adrenal neuro-immune crosstalk.

Multiple GPCR's are coupled to $[Ca^{2+}]_i$ release in macrophages in the adrenal medulla

An emerging feature of macrophage biology is the realization that tissue resident macrophages are adapted to their local environment. For example, peripheral nerve-associated macrophages have a transcriptional profile that distinguishes them from macrophages in the CNS or peritoneal cavity (Gainullina et al., 2023; Wang et al., 2020). This suggests that medulla macrophages might respond to modulators relevant to autonomic function. With this in mind, I monitored the levels of intracellular calcium in medulla macrophages in adrenal slices and quantified the response to agonist application. Adrenal sections were prepared from Lyz2cre-GCaMP6f-tdTomato mice. Cells expressing the GCaMP6f calcium sensor (identified by the co-expression of tdTomato) were present throughout the adrenal. To determine which medulla cell types were labelled, adrenal sections were co-stained for RFP and immune cell markers. This showed that 98% of RFP-ir cells in the medulla were CD45-ir, indicating that RFP (and thus GCaMP6f) expression was restricted to immune cells. Conversely, 80% of CD45-ir cells were RFP positive (Fig 6A). Thus, there are some immune cells in the medulla that do not express Lyz2-cre, possibly T cells or B cells (Dolfi et al., 2022). Next, to examine what fraction of the RFP cells were macrophages, sections were co-stained for RFP and F4/80 (Fig 6A). Quantification of the staining indicated that 88% of the RFP-ir cells in the medulla were F4/80-ir. Conversely, 98% of medulla F4/80-ir cells were also RFP positive. Thus, all medulla macrophages/monocytes express RFP / GCaMP6f (Fig 6A) but there is a small population of Lyz2-cre positive cells (~12%) that express RFP / GCaMP6f but are F4/80 negative. The

identity of these Lyz2-cre expressing cells is not known but could include granulocytes, dendritic cells or innate lymphoid cells (Dolfi et al., 2022; Shi et al., 2018).

Lyz2-cre expression has also been reported in some neuronal cells (Orthgiess et al., 2016). To determine if this occurred in the adrenal, sections were co-stained for the neuronal marker, MAP2 and RFP. As shown in Extended Data Fig 6-2, in addition to the neuroendocrine chromaffin cells which are MAP2-ir, the adrenal contained MAP2-ir processes in the capsule, cortex and medulla. The processes in the medulla are likely to arise from intra-adrenal ganglion neurons or sensory afferents (Dagerlind et al., 1995; Mohamed et al., 1988). However, the MAP2-ir did not co-localize with RFP. Finally, to directly express GCaMP6f in chromaffin cells I generated an NPYcre-GCaMP6f-tdTomato mouse line (NPY is expressed by all mouse chromaffin cells; (Wang et al., 2013)). As shown in Extended Data Fig 6-1E,F, RFP was present throughout the medulla in cells with the distinctive morphology of chromaffin cells. Thus, in the adrenal medulla of Lyz2cre-GCaMP6f-tdTomato mice, RFP (and GCaMP6f) expression is effectively restricted to hematopoietic (CD45-ir) cells and is not present in neurons or neuroendocrine chromaffin cells.

Next, calcium levels were measured in individual cells in adrenal slices from Lyz2cre-GCaMP6f-tdTomato mice. Under basal conditions, calcium levels were stable and spontaneous transients were rarely seen. I initially examined the response to purinergic agonists because ATP is a transmitter that is released from chromaffin cells (Hollins and Ikeda, 1997; Zhang et al., 2019) and P2Y receptors are widely expressed in macrophages (Lovászi et al., 2021). ATP had only modest effects on $[Ca^{2+}]_i$, but application of UDP (an agonist of P2Y6 and P2Y14 receptors) consistently increased calcium levels in adrenal macrophages (Fig 6B). Only a few cells responded to UDP-glucose (P2Y14 agonist) while the actions of UTP were comparable to UDP. Other purinergic agonists, adenosine and ADP were ineffective (Fig 6B). The response to 100 µM UDP was inhibited by the P2Y receptor antagonist reactive blue-2 (Fig 6C). This pharmacological profile is consistent with expression of the P2Y6 receptor (Jacobson et al., 2020) in adrenal medulla macrophages, in agreement with RNAseq studies (Bedoya-Reina et al., 2021; Dolfi et al., 2022).

Acetylcholine is the classical transmitter released from preganglionic neurons that innervate chromaffin cells (Barbara and Takeda, 1996). Application of 100 µM and 1 mM ACh both generated a biphasic increase in $[Ca^{2+}]_i$ in adrenal macrophages (Fig 7A and Extended Data 7-1A,B). Agonists of nACh receptors including dimethylphenylpiperazinium (DMPP), which is widely used to activate adrenal nAChR's (Brindley et al., 2017; Chen et al., 2024; Maldifassi et al., 2024), were particularly effective (Fig 7A and Extended Data 7-1C,D). Oxotremorine-M (a muscarinic agonist) also increased $[Ca^{2+}]_i$ (Fig 7A). The effect of ACh and Oxotremorine-M decremented with repeated application, but the response to DMPP was blocked by the nicotinic antagonist mecamylamine (Extended Data Fig 7-1C,D) confirming the effect was mediated by nACh receptors. PACAP, a preganglionic peptide co-transmitter (Kumar et al., 2010) also increased $[Ca^{2+}]_i$ in adrenal macrophages (Fig 7A). In contrast, modulators released by chromaffin cells (norepinephrine, NPY and met-enkephalin), sensory neurons (substance P) and multiple cell types (LPA and glutamate) were without effect (Fig 7A and Extended Data Fig 7-1D). GABA which is synthesized and released from chromaffin cells (Inoue et al., 2010) had a small but consistent effect (Extended Data Fig 7-1D). The vasoactive hormones, angiotensin II and bradykinin, both increased $[Ca^{2+}]_i$ in medulla macrophages (Fig 7A).

Finally, application of histamine also reliably increased $[Ca^{2+}]_i$ (Fig 7A) in medulla macrophages with a threshold dose of ~ 100 nM (Fig 7B). The effect of histamine was mediated by H1 receptors because it was blocked by pyrilamine maleate but not by cimetidine, an H2 receptor antagonist (Fig 7C). The histamine-induced increase in $[Ca^{2+}]_i$ was biphasic with a rapid initial peak and slower second phase (Fig 7C,D). Removal of extracellular calcium reduced the amplitude of both phases (Fig 7D) consistent with the involvement of both calcium influx and release from internal stores. When calcium was returned to the bathing medium there was a large rebound increase in $[Ca^{2+}]_i$ which is characteristic of store-operated calcium entry (Fig 7D).

The robust response of adrenal macrophages to ACh and multiple GPCR (G protein-coupled receptor) agonists was unexpected. However, because the adrenal is composed of numerous cell types, it is possible that these effects are mediated indirectly. I examined this issue in two ways. First, I minimized the contribution of other cells by dissociating adrenal tissue from Lyz2cre-GCaMP6f mice and examined the response of tdTomato-expressing cells *in vitro*. Four agonists were tested that either evoked responses ex vivo (UTP, histamine and ACh) or were expected to do so (ATP). Application of UDP and ATP increased $[Ca^{2+}]_i$, but surprisingly, histamine and acetylcholine were now ineffective (Fig 8A, histamine P = 0.239; ACh P = 0.233; one sample T test). Curiously, ATP reliably increased $[Ca^{2+}]_i$ *in vitro* in contrast to the results in slices (compare Fig 6B and Fig 8A), perhaps because the cultured cells are a mix of cortical and medulla macrophages (autofluorescence prevented quantification of $[Ca^{2+}]_i$ in cortical macrophages in slices). Second, I tested whether other peripheral macrophages showed similar responses to the same agonists. Both peritoneal and pulmonary macrophages from Lyz2cre-GCaMP6f mice responded to UDP and ATP but not to ACh or histamine (Fig 8B,C). These results confirm that UDP (and ATP) act directly on adrenal macrophages, but the effect of histamine (and perhaps ACh) are likely mediated *via* an intervening cell type(s).

DISCUSSION

While it is accepted that the adrenal gland contains multiple types of immune cells, their zonal location and function is less clear. This issue is significant because the adrenal is broadly composed of two regions, an outer cortex containing endocrine cells and an inner medulla that is neuroendocrine and part of the sympathetic nervous system. Given the function of these regions is specialized it seems likely that the functions of the resident immune cells will also be distinct. As an initial step towards understanding their role in adrenal physiology, I investigated immune cell distribution in the mouse adrenal medulla and the response to a range of adrenal-relevant neuromodulators (Carbone et al., 2019). This region of the gland was found to contain a large population of CD45-immunoreactive myeloid cells, most of which appear to be F4/80+/Lyz2+ macrophages. These cells are found throughout the gland, but within the medulla they reside close to multiple cell types including chromaffin cells, endothelial cells, satellite glial cells and presumptive pre-ganglionic axons. Thus, like the CNS which contains microglia, the neuroendocrine component of the adrenal gland is also populated with resident macrophages. This finding confirms earlier studies in both rodents and humans which showed that macrophages are present within all four adrenal zones (Engström et al., 2008; González-Hernández et al., 1994; Hume et al., 1984; Sato, 1998; Schober et al., 1998). A recent RNAseq study of mouse adrenal gland immune cells identified 4 macrophage populations but whether there is a medulla-specific population is not known (Dolfi et al., 2022).

Monitoring the levels of intracellular calcium in medulla macrophages using Lyz2cre-GCaMP6f mice, showed these cells can respond to a wide variety of modulators that are generated within the gland or found within the systemic circulation. In common with many macrophage populations (del Rey et al., 2006; Gryshchenko et al., 2021; Hanley et al., 2004; Koizumi et al., 2007; Weitz et al., 2018), those within the medulla are sensitive to multiple purinergic agonists. In slices, the largest effects were to uridine nucleotides. Combined with the modest response to adenosine nucleotides, the receptor most likely to be responsible is P2Y6 and this is also consistent with inhibition of the UDP-evoked response by reactive blue-2 (although it is acknowledged that some agonists were only tested at a single concentration). P2Y6 receptors are expressed by a diversity of macrophages including microglia and peritoneal macrophages (Bar et al., 2008; del Rey et al., 2006; Koizumi et al., 2007; Morioka et al., 2013). In microglia, activation of P2Y6 receptors by UDP released from damaged neurons increases microglial phagocytosis (Koizumi et al., 2007). Although this pathway could also be active in the adrenal, chromaffin cells release ATP as a co-transmitter (Hollins and Ikeda, 1997; Zhang et al., 2019) and UTP and UDP are found in dense core secretory granules in chromaffin cells (Bankston and Guidotti, 1996; Van Dyke et al., 1977). Thus, medulla macrophages are likely to be exposed to high concentrations of secreted purines under physiological levels of sympathetic activity. Unexpectedly ATP had little effect on $[Ca]_i$ on adrenal macrophages in slices but evoked a substantial response *in vitro*. The reason for this is not known. One possibility is that in the slice, macrophage receptors are partially desensitized due to tonic ATP release from chromaffin cells. Another possibility is that ATP primarily acts as a paracrine factor on chromaffin cells rather than on macrophages. Finally, CNS macrophages (microglia) show rapid transcriptional changes when placed *in vitro* (Bohlen et al., 2017) and thus there may not be a complete correspondence between the responses of macrophages *in vitro* and in the adrenal slice.

A number of other agonists also effectively increased calcium in medulla macrophages including ACh and PACAP which are classical and peptidergic co-transmitters respectively, released by the pre-ganglionic neurons that innervate chromaffin cells (Barbara and Takeda, 1996; Inoue et al., 2000; Kumar et al., 2010). Curiously the response to ACh was absent when adrenal macrophages were isolated *in vitro*. This suggests that the receptors are either rapidly lost when the cells were placed in culture or that the actions of ACh are mediated *via* an intervening cell type. A similar discrepancy was noted for histamine which robustly increased calcium in medulla macrophages in adrenal slices but had no significant effect on adrenal macrophages *in vitro*. The identity of a putative intervening cell type(s) is unknown, although chromaffin cells are plausible candidates since they express nicotinic and muscarinic ACh receptors (Akaike et al., 1990; Barbara et al., 1998; Barbara and Takeda, 1996; Colomer et al., 2010). Suggestively, chromaffin cells also express H1 histamine receptors, the same subtype involved in the macrophage response to histamine (Borges, 1994; Currie and Fox, 2000; Marley et al., 1991). Endogenous sources of ACh include the sympathetic preganglionic neurons (Barbara and Takeda, 1996). Histamine is not known to be secreted from preganglionic neurons but has been reported in chromaffin cells (Häppölä et al., 1985; Tuominen et al., 1993). Mast cells are present in the adrenal, but these are in the cortex (Boyer et al., 2017; Kim et al., 1997) and so unlikely to supply histamine to macrophages in the medulla. Staining for c-kit, a marker of mast cells (Tauber et al., 2023), confirmed these cells are absent from the mouse adrenal medulla (not shown). Previous work has also suggested that a likely origin of histamine within the adrenal is entry from the systemic circulation (Borges, 1994). The threshold dose for the histamine-

induced increase in cytoplasmic calcium in medulla macrophages was ~ 100 nM. Systemic levels of histamine are in the low nM range although they can rise several fold during an inflammatory response (Boehm et al., 2019; Shiva et al., 2008).

Although the role of the medulla macrophages remains to be determined, their close association with the pre-ganglionic input and the post-ganglionic chromaffin cells raises the possibility they modulate sympatho-adrenal activity. Conceivably this could occur during a classical immune response (such as infection), under fight-or-flight conditions (such as chronic stress) or on a developmental time scale (such as synaptic pruning). Macrophages are known to be involved in all of these contexts (Biltz et al., 2022; Meroni et al., 2019; Pavlov et al., 2018; Wolf et al., 2017). The mechanism(s) underlying this communication is not clear but adrenal macrophages can synthesize a variety of cytokines, including IL-1β, TNFα, TGF-β and other inflammatory molecules (Engström et al., 2008; González-Hernández et al., 1996; Xu et al., 2024). Many of these signaling molecules regulate the synthesis and release of catecholamines and neuropeptides from chromaffin cells (Carbone et al., 2019; Douglas et al., 2010; Jewell et al., 2011; Rosmaninho-Salgado et al., 2009).

Finally, although macrophages are distributed throughout the adrenal medulla they were often associated with axonal processes (Fig 4B). This is reminiscent of the nerve associated macrophages (NAM's) that are found in the lungs (Ural et al., 2020), adipose tissue (Pirzgalska et al., 2017), skin (Kolter et al., 2019) and GI tract (Muller et al., 2014). In future work it will be informative to test whether adrenal macrophages are able to acutely modulate epinephrine release and sympatho-adrenal function.

REFERENCES

Akaike A, Mine Y, Sasa M, Takaori S (1990) Voltage and current clamp studies of muscarinic and nicotinic excitation of the rat adrenal chromaffin cells. J Pharmacol Exp Ther 255:333–339.

Avraham O, Deng P-Y, Jones S, Kuruvilla R, Semenkovich CF, Klyachko VA, Cavalli V (2020) Satellite glial cells promote regenerative growth in sensory neurons. Nat Commun 11:4891.

Bankston LA, Guidotti G (1996) Characterization of ATP transport into chromaffin granule ghosts. Synergy of ATP and serotonin accumulation in chromaffin granule ghosts. J Biol Chem 271:17132–17138.

Bar I, Guns P-J, Metallo J, Cammarata D, Wilkin F, Boeynams J-M, Bult H, Robaye B (2008) Knockout mice reveal a role for P2Y6 receptor in macrophages, endothelial cells, and vascular smooth muscle cells. Mol Pharmacol 74:777–784.

Barbara JG, Lemos VS, Takeda K (1998) Pre- and post-synaptic muscarinic receptors in thin slices of rat adrenal gland. Eur J Neurosci 10:3535–3545.

Barbara JG, Takeda K (1996) Quantal release at a neuronal nicotinic synapse from rat adrenal gland. Proc Natl Acad Sci USA 93:9905–9909.

Bedoya-Reina OC, Li W, Arceo M, Plescher M, Bullova P, Pui H, Kaucka M, Kharchenko P, Martinsson T, Holmberg J, Adameyko I, Deng Q, Larsson C, Juhlin CC, Kogner P, Schlisio S (2021) Single-nuclei transcriptomes from human adrenal gland reveal distinct cellular identities of low and high-risk neuroblastoma tumors. Nat Commun 12:5309.

Biltz RG, Sawicki CM, Sheridan JF, Godbout JP (2022) The neuroimmunology of social-stress-induced sensitization. Nat Immunol 23:1527–1535.

Boehm T, Reiter B, Ristl R, Petroczi K, Sperr W, Stimpfl T, Valent P, Jilma B (2019) Massive release of the histamine-degrading enzyme diamine oxidase during severe anaphylaxis in mastocytosis patients. Allergy 74:583–593.

Bohlen CJ, Bennett FC, Tucker AF, Collins HY, Mulinyawe SB, Barres BA (2017) Diverse Requirements for Microglial Survival, Specification, and Function Revealed by Defined-Medium Cultures. Neuron 94:759-773.e8.

Borges R (1994) Histamine H1 receptor activation mediates the preferential release of adrenaline in the rat adrenal gland. Life Sci 54:631–640.

Boyer H-G, Wils J, Renouf S, Arabo A, Duparc C, Boutelet I, Lefebvre H, Louiset E (2017) Dysregulation of Aldosterone Secretion in Mast Cell-Deficient Mice. Hypertension 70:1256–1263.

Brindley RL, Bauer MB, Hartley ND, Horning KJ, Currie KPM (2017) Sigma-1 receptor ligands inhibit catecholamine secretion from adrenal chromaffin cells due to block of nicotinic acetylcholine receptors. J Neurochem 143:171–182.

Cambray-Deakin MA, Burgoyne RD (1987) Posttranslational modifications of alpha-tubulin: acetylated and detyrosinated forms in axons of rat cerebellum. J Cell Biol 104:1569–1574.

Carbone E, Borges R, Eiden LE, García AG, Hernández-Cruz A (2019) Chromaffin Cells of the Adrenal Medulla: Physiology, Pharmacology, and Disease. Compr Physiol 9:1443–1502.
Chen X, Bell NA, Coffman BL, Rabino AA, Garcia-Mata R, Kammermeier PJ, Yule DI, Axelrod D, Smrcka AV, Giovannucci DR, Anantharam A (2024) A PACAP-activated network for secretion requires coordination of Ca2+ influx and Ca2+ mobilization. Mol Biol Cell 35:ar92.
Clausen BE, Burkhardt C, Reith W, Renkawitz R, Förster I (1999) Conditional gene targeting in macrophages and granulocytes using LysMcre mice. Transgenic Res 8:265–277.
Colomer C, Olivos-Oré LA, Vincent A, McIntosh JM, Artalejo AR, Guérineau NC (2010) Functional characterization of alpha9-containing cholinergic nicotinic receptors in the rat adrenal medulla: implication in stress-induced functional plasticity. J Neurosci 30:6732–6742.
Coupland RE, Parker TL, Kesse WK, Mohamed AA (1989) The innervation of the adrenal gland. III. Vagal innervation. J Anat 163:173–181.
Cryer PE (1993) Glucose counterregulation: prevention and correction of hypoglycemia in humans. Am J Physiol 264:E149-155.
Currie KP, Fox AP (2000) Voltage-dependent, pertussis toxin insensitive inhibition of calcium currents by histamine in bovine adrenal chromaffin cells. J Neurophysiol 83:1435–1442.
Currie KP, Zhou Z, Fox AP (2000) Evidence for paracrine signaling between macrophages and bovine adrenal chromaffin cell Ca(2+) channels. J Neurophysiol 83:280–287.
Dagerlind A, Pelto-Huikko M, Diez M, Hökfelt T (1995) Adrenal medullary ganglion neurons project into the splanchnic nerve. Neuroscience 69:1019–1023.
del Rey A, Renigunta V, Dalpke AH, Leipziger J, Matos JE, Robaye B, Zuzarte M, Kavelaars A, Hanley PJ (2006) Knock-out mice reveal the contributions of P2Y and P2X receptors to nucleotide-induced Ca2+ signaling in macrophages. J Biol Chem 281:35147–35155.
Dolfi B et al. (2022) Unravelling the sex-specific diversity and functions of adrenal gland macrophages. Cell Rep 39:110949.
Dong TX, Othy S, Jairaman A, Skupsky J, Zavala A, Parker I, Dynes JL, Cahalan MD (2017) T-cell calcium dynamics visualized in a ratiometric tdTomato-GCaMP6f transgenic reporter mouse. Elife 6:e32417.
Douglas SA, Bunn SJ (2009) Interferon-alpha signalling in bovine adrenal chromaffin cells: involvement of signal-transducer and activator of transcription 1 and 2, extracellular signal-regulated protein kinases 1/2 and serine 31 phosphorylation of tyrosine hydroxylase. J Neuroendocrinol 21:200–207.
Douglas SA, Sreenivasan D, Carman FH, Bunn SJ (2010) Cytokine interactions with adrenal medullary chromaffin cells. Cell Mol Neurobiol 30:1467–1475.
Engström L, Rosén K, Angel A, Fyrberg A, Mackerlova L, Konsman JP, Engblom D, Blomqvist A (2008) Systemic immune challenge activates an intrinsically regulated local inflammatory circuit in the adrenal gland. Endocrinology 149:1436–1450.
Gainullina A et al. (2023) Network analysis of large-scale ImmGen and Tabula Muris datasets highlights metabolic diversity of tissue mononuclear phagocytes. Cell Rep 42:112046.
Gautron L, Rutkowski JM, Burton MD, Wei W, Wan Y, Elmquist JK (2013) Neuronal and nonneuronal cholinergic structures in the mouse gastrointestinal tract and spleen. J Comp Neurol 521:3741–3767.
Glynn MW, McAllister AK (2006) Immunocytochemistry and quantification of protein colocalization in cultured neurons. Nat Protoc 1:1287–1296.
González-Hernández JA, Bornstein SR, Ehrhart-Bornstein M, Geschwend JE, Adler G, Scherbaum WA (1994) Macrophages within the human adrenal gland. Cell Tissue Res 278:201–205.
González-Hernández JA, Ehrhart-Bornstein M, Späth-Schwalbe E, Scherbaum WA, Bornstein SR (1996) Human adrenal cells express tumor necrosis factor-alpha messenger

ribonucleic acid: evidence for paracrine control of adrenal function. J Clin Endocrinol Metab 81:807–813.
Gryshchenko O, Gerasimenko JV, Petersen OH, Gerasimenko OV (2021) Calcium Signaling in Pancreatic Immune Cells In situ. Function (Oxf) 2:zqaa026.
Hanani M, Spray DC (2020) Emerging importance of satellite glia in nervous system function and dysfunction. Nat Rev Neurosci 21:485–498.
Hanley PJ, Musset B, Renigunta V, Limberg SH, Dalpke AH, Sus R, Heeg KM, Preisig-Müller R, Daut J (2004) Extracellular ATP induces oscillations of intracellular Ca2+ and membrane potential and promotes transcription of IL-6 in macrophages. Proc Natl Acad Sci U S A 101:9479–9484.
Häppölä O, Soinila S, Päivärinta H, Joh TH, Panula P (1985) Histamine-immunoreactive endocrine cells in the adrenal medulla of the rat. Brain Res 339:393–396.
Hershkovitz L, Beuschlein F, Klammer S, Krup M, Weinstein Y (2007) Adrenal 20alpha-hydroxysteroid dehydrogenase in the mouse catabolizes progesterone and 11-deoxycorticosterone and is restricted to the X-zone. Endocrinology 148:976–988.
Hollins B, Ikeda SR (1997) Heterologous expression of a P2x-purinoceptor in rat chromaffin cells detects vesicular ATP release. J Neurophysiol 78:3069–3076.
Hume DA (2011) Applications of myeloid-specific promoters in transgenic mice support in vivo imaging and functional genomics but do not support the concept of distinct macrophage and dendritic cell lineages or roles in immunity. J Leukoc Biol 89:525–538.
Hume DA, Halpin D, Charlton H, Gordon S (1984) The mononuclear phagocyte system of the mouse defined by immunohistochemical localization of antigen F4/80: macrophages of endocrine organs. Proc Natl Acad Sci U S A 81:4174–4177.
Inoue M, Fujishiro N, Ogawa K, Muroi M, Sakamoto Y, Imanaga I, Shioda S (2000) Pituitary adenylate cyclase-activating polypeptide may function as a neuromodulator in guinea-pig adrenal medulla. J Physiol 528:473–487.
Inoue M, Harada K, Matsuoka H, Warashina A (2010) Paracrine role of GABA in adrenal chromaffin cells. Cell Mol Neurobiol 30:1217–1224.
Jacobson KA, Delicado EG, Gachet C, Kennedy C, von Kügelgen I, Li B, Miras-Portugal MT, Novak I, Schöneberg T, Perez-Sen R, Thor D, Wu B, Yang Z, Müller CE (2020) Update of P2Y receptor pharmacology: IUPHAR Review 27. Br J Pharmacol 177:2413–2433.
Jewell ML, Breyer RM, Currie KPM (2011) Regulation of calcium channels and exocytosis in mouse adrenal chromaffin cells by prostaglandin EP3 receptors. Mol Pharmacol 79:987–996.
Jones SB, Wang Z, Wang X, Roberts JC, Weber M, Mathews HL (1993) Immune cells mediate epinephrine secretion from bovine chromaffin cells in vitro. Life Sci 53:PL447-451.
Katkar G, Ghosh P (2023) Macrophage states: there's a method in the madness. Trends Immunol 44:954–964.
Kesse WK, Parker TL, Coupland RE (1988) The innervation of the adrenal gland. I. The source of pre- and postganglionic nerve fibres to the rat adrenal gland. J Anat 157:33–41.
Kim JS, Kubota H, Kiuchi Y, Doi K, Saegusa J (1997) Subcapsular cell hyperplasia and mast cell infiltration in the adrenal cortex of mice: comparative study in 7 inbred strains. Exp Anim 46:303–306.
Klein Wolterink RGJ, Wu GS, Chiu IM, Veiga-Fernandes H (2022) Neuroimmune Interactions in Peripheral Organs. Annu Rev Neurosci 45:339–360.
Koizumi S, Shigemoto-Mogami Y, Nasu-Tada K, Shinozaki Y, Ohsawa K, Tsuda M, Joshi BV, Jacobson KA, Kohsaka S, Inoue K (2007) UDP acting at P2Y6 receptors is a mediator of microglial phagocytosis. Nature 446:1091–1095.
Kolter J, Feuerstein R, Zeis P, Hagemeyer N, Paterson N, d'Errico P, Baasch S, Amann L, Masuda T, Lösslein A, Gharun K, Meyer-Luehmann M, Waskow C, Franzke C-W, Grün D, Lämmermann T, Prinz M, Henneke P (2019) A Subset of Skin Macrophages

Contributes to the Surveillance and Regeneration of Local Nerves. Immunity 50:1482-1497.e7.
Kumar NN, Allen K, Parker L, Damanhuri H, Goodchild AK (2010) Neuropeptide coding of sympathetic preganglionic neurons; focus on adrenally projecting populations. Neuroscience 170:789–799.
Kvetnanský R, Nankova B, Hiremagalur B, Viskupic E, Vietor I, Rusnak M, McMahon A, Kopin IJ, Sabban EL (1996) Induction of adrenal tyrosine hydroxylase mRNA by single immobilization stress occurs even after splanchnic transection and in the presence of cholinergic antagonists. J Neurochem 66:138–146.
Lamarche L, Yamaguchi N, Péronnet F, Guitard F (1992) Evidence against a humoral control mechanism in adrenal catecholamine secretion during insulin-induced hypoglycemia. Am J Physiol 262:R659-665.
Lovászi M, Branco Haas C, Antonioli L, Pacher P, Haskó G (2021) The role of P2Y receptors in regulating immunity and metabolism. Biochem Pharmacol 187:114419.
Lujan HJ, Mathews HL, Gamelli RL, Jones SB (1998) Human immune cells mediate catecholamine secretion from adrenal chromaffin cells. Crit Care Med 26:1218–1224.
Ma Y, Wang Q, Joe D, Wang M, Whim MD (2018) Recurrent hypoglycemia inhibits the counterregulatory response by suppressing adrenal activity. J Clin Invest 128:3866–3871.
Maldifassi MC, Guerra-Fernández MJ, Ponce D, Alfonso-Bueno S, Maripillán J, Vielma AH, Báez-Matus X, Marengo FD, Acuña-Castillo C, Sáez JC, Martínez AD, Cárdenas AM (2024) Autocrine activation of P2X7 receptors mediates catecholamine secretion in chromaffin cells. Br J Pharmacol 181:2905–2922.
Marley PD, Thomson KA, Jachno K, Johnston MJ (1991) Histamine-induced increases in cyclic AMP levels in bovine adrenal medullary cells. Br J Pharmacol 104:839–846.
McKinley MJ, Martelli D, Trevizan-Baú P, McAllen RM (2022) Divergent splanchnic sympathetic efferent nerve pathways regulate interleukin-10 and tumour necrosis factor-α responses to endotoxaemia. J Physiol 600:4521–4536.
Meroni E, Stakenborg N, Viola MF, Boeckxstaens GE (2019) Intestinal macrophages and their interaction with the enteric nervous system in health and inflammatory bowel disease. Acta Physiol (Oxf) 225:e13163.
Milstein AD, Bloss EB, Apostolides PF, Vaidya SP, Dilly GA, Zemelman BV, Magee JC (2015) Inhibitory Gating of Input Comparison in the CA1 Microcircuit. Neuron 87:1274–1289.
Mohamed AA, Parker TL, Coupland RE (1988) The innervation of the adrenal gland. II. The source of spinal afferent nerve fibres to the guinea-pig adrenal gland. J Anat 160:51–58.
Morioka N, Tokuhara M, Harano S, Nakamura Y, Hisaoka-Nakashima K, Nakata Y (2013) The activation of P2Y6 receptor in cultured spinal microglia induces the production of CCL2 through the MAP kinases-NF-κB pathway. Neuropharmacology 75:116–125.
Muller PA, Koscsó B, Rajani GM, Stevanovic K, Berres M-L, Hashimoto D, Mortha A, Leboeuf M, Li X-M, Mucida D, Stanley ER, Dahan S, Margolis KG, Gershon MD, Merad M, Bogunovic M (2014) Crosstalk between muscularis macrophages and enteric neurons regulates gastrointestinal motility. Cell 158:300–313.
Orthgiess J, Gericke M, Immig K, Schulz A, Hirrlinger J, Bechmann I, Eilers J (2016) Neurons exhibit Lyz2 promoter activity in vivo: Implications for using LysM-Cre mice in myeloid cell research. Eur J Immunol 46:1529–1532.
Pavlov VA, Chavan SS, Tracey KJ (2018) Molecular and Functional Neuroscience in Immunity. Annu Rev Immunol 36:783–812.
Pirzgalska RM et al. (2017) Sympathetic neuron-associated macrophages contribute to obesity by importing and metabolizing norepinephrine. Nat Med 23:1309–1318.
Roberts JC, Jones SB (1997) Chromaffin cell epinephrine secretion mediated by a macrophage peptide: the role of endotoxin. Shock 7:211–216.

Roberts JC, Mathews HL, DePotter W, Pinxteren J, Jones SB (1996) Mononuclear-cell peptide mediation of chromaffin-cell epinephrine secretion. Neuroimmunomodulation 3:119–130.
Rosmaninho-Salgado J, Araújo IM, Alvaro AR, Mendes AF, Ferreira L, Grouzmann E, Mota A, Duarte EP, Cavadas C (2009) Regulation of catecholamine release and tyrosine hydroxylase in human adrenal chromaffin cells by interleukin-1beta: role of neuropeptide Y and nitric oxide. J Neurochem 109:911–922.
Sato T (1998) Class II MHC-expressing cells in the rat adrenal gland defined by monoclonal antibodies. Histochem Cell Biol 109:359–367.
Schindelin J, Arganda-Carreras I, Frise E, Kaynig V, Longair M, Pietzsch T, Preibisch S, Rueden C, Saalfeld S, Schmid B, Tinevez J-Y, White DJ, Hartenstein V, Eliceiri K, Tomancak P, Cardona A (2012) Fiji: an open-source platform for biological-image analysis. Nat Methods 9:676–682.
Schober A, Huber K, Fey J, Unsicker K (1998) Distinct populations of macrophages in the adult rat adrenal gland: a subpopulation with neurotrophin-4-like immunoreactivity. Cell Tissue Res 291:365–373.
Shi J, Hua L, Harmer D, Li P, Ren G (2018) Cre Driver Mice Targeting Macrophages. Methods Mol Biol 1784:263–275.
Shiva D, Matsumoto T, Kremenik MJ, Kato Y, Yano H (2008) High dose of lipopolysaccharide pre-treatment prevents OVA-induced anaphylactic decreases in rectal temperature in the immunized mice. Immunol Lett 118:59–64.
Stanley S, Moheet A, Seaquist ER (2019) Central Mechanisms of Glucose Sensing and Counterregulation in Defense of Hypoglycemia. Endocr Rev 40:768–788.
Tauber M et al. (2023) Landscape of mast cell populations across organs in mice and humans. J Exp Med 220:e20230570.
Tuominen RK, Karhunen T, Panula P, Yamatodani A (1993) Endogenous histamine in cultured bovine adrenal chromaffin cells. Eur J Neurosci 5:1436–1441.
Ural BB, Yeung ST, Damani-Yokota P, Devlin JC, de Vries M, Vera-Licona P, Samji T, Sawai CM, Jang G, Perez OA, Pham Q, Maher L, Loke P, Dittmann M, Reizis B, Khanna KM (2020) Identification of a nerve-associated, lung-resident interstitial macrophage subset with distinct localization and immunoregulatory properties. Sci Immunol 5:eaax8756.
Van Dyke K, Robinson R, Urquilla P, Smith D, Taylor M, Trush M, Wilson M (1977) An analysis of nucleotides and catecholamines in bovine medullary granules by anion exchange high pressure liquid chromatography and fluorescence. Evidence that most of the catecholamines in chromaffin granules are stored without associated ATP. Pharmacology 15:377–391.
Wang M, Wang Q, Whim MD (2016) Fasting induces a form of autonomic synaptic plasticity that prevents hypoglycemia. Proc Natl Acad Sci USA 113:E3029-3038.
Wang PL, Yim AKY, Kim K-W, Avey D, Czepielewski RS, Colonna M, Milbrandt J, Randolph GJ (2020) Peripheral nerve resident macrophages share tissue-specific programming and features of activated microglia. Nat Commun 11:2552.
Wang Q, Wang M, Whim MD (2013) Neuropeptide y gates a stress-induced, long-lasting plasticity in the sympathetic nervous system. J Neurosci 33:12705–12717.
Wang Z et al. (2023) An immune cell atlas reveals the dynamics of human macrophage specification during prenatal development. Cell 186:4454-4471.e19.
Watson RE, Wiegand SJ, Clough RW, Hoffman GE (1986) Use of cryoprotectant to maintain long-term peptide immunoreactivity and tissue morphology. Peptides 7:155–159.
Weitz JR, Makhmutova M, Almaça J, Stertmann J, Aamodt K, Brissova M, Speier S, Rodriguez-Diaz R, Caicedo A (2018) Mouse pancreatic islet macrophages use locally released ATP to monitor beta cell activity. Diabetologia 61:182–192.
Whim MD (2006) Near simultaneous release of classical and peptide cotransmitters from chromaffin cells. J Neurosci 26:6637–6642.

Wolf Y, Boura-Halfon S, Cortese N, Haimon Z, Sar Shalom H, Kuperman Y, Kalchenko V, Brandis A, David E, Segal-Hayoun Y, Chappell-Maor L, Yaron A, Jung S (2017) Brown-adipose-tissue macrophages control tissue innervation and homeostatic energy expenditure. Nat Immunol 18:665–674.

Xu Y, Patterson MT, Dolfi B, Zhu A, Bertola A, Schrank PR, Gallerand A, Kennedy AE, Hillman H, Dinh L, Shekhar S, Tollison S, Bold TD, Ivanov S, Williams JW (2024) Adrenal gland macrophages regulate glucocorticoid production through Trem2 and TGF-β. JCI Insight 9:e174746.

Zhang Q et al. (2019) Differential Co-release of Two Neurotransmitters from a Vesicle Fusion Pore in Mammalian Adrenal Chromaffin Cells. Neuron 102:173-183.e4.

Zhou XF, Oldfield BJ, Livett BG (1991) Substance P-containing sensory neurons in the rat dorsal root ganglia innervate the adrenal medulla. J Auton Nerv Syst 33:247–254.

Zhou ZZ, Jones SB (1993) Involvement of central vs. peripheral mechanisms in mediating sympathoadrenal activation in endotoxic rats. Am J Physiol 265:R683-688.

FIGURE LEGENDS

Figure 1. Immune cells are distributed throughout the mouse adrenal gland. A. CD45-immunoreactive myeloid cells are present in the cortex (Crtx) and medulla (Med) of the adrenal gland. B. In the medulla, the majority of CD45-ir cells are elongated with fine processes. C. An example of a rare spherical CD45-ir cell in the medulla. ZG zona glomerulosa; ZF zona fasciculata. Scale bar 200 µm (A); 20 µm (B,C).

Figure 2. Cells in the adrenal medulla are labelled with a variety of macrophage markers. A. F4/80-ir cells are present in the adrenal cortex (Crtx) and medulla (Med). F4/80-ir labels a band of cells in the cortical X-zone (xz; open arrowhead) and cells throughout the medulla (closed arrow heads). B. Higher magnification of F4/80-ir cells in the medulla indicates the cells are elongate with fine processes. C. CD68-ir cells are prominent in the X-zone and also present in the medulla. D. CD301-ir cells are located in the capsule / zona glomerulosa and medulla. E. CD115-ir cells are located in the cortex and sparse in the medulla. F. MHC II-ir cells are primarily located in the outer cortex. G. Macrophages that are Iba-ir are present throughout the adrenal including the medulla. H. Lysozyme2-expressing cells (Lyz2) labelled with tdTomato (Lyz2cre-GCaMP6f mouse) are present in an inner cortical region and throughout the adrenal medulla. Scale bar 100 µm (A, C-H); 20 µm (B). See also Extended Data Figure 2-1 for more details.

Figure 3. Macrophages in the adrenal medulla are closely associated with multiple cell types. A, B. F4/80-ir cells in the medulla are intermingled with tyrosine hydroxylase-ir chromaffin cells. C, D. F4/80-ir macrophages are juxtaposed to PNMT-ir (white arrowheads) and PNMT-negative chromaffin cells (red arrowheads). E, F. F4/80-ir cells are located next to chromaffin cells that are NPY-ir. G, H. F4/80-ir cells (white arrowheads) are close to GFAP-ir satellite glial cells in the medulla. Note also a band of GFAP-ir cells is located in the adrenal capsule (green arrowheads). I, J. Some Lyz2-expressing cells (white arrowheads) are close to CD31-ir endothelial cells in the medulla. Scale bar 100 µm (A, C, E, G, I); 20 µm (B, D, F, H, J). See also Extended Data Figure 3-1 for more details.

Figure 4. Nerve-associated macrophages in the adrenal medulla. A, B. Staining for an axonal marker (acetylated tubulin, acTub) reveals dense labelling throughout the medulla. Co-localization with F4/80-ir shows that macrophages are associated with acTub-ir axonal processes and often aligned (white circles). C, D. Synapsin-ir synaptic varicosities are densely distributed throughout the adrenal medulla. Higher magnification reveals potential sites of interaction with F4/80-ir macrophages in the medulla (white circles). Scale bar 100 µm (A, C); 20 µm (B, D).

Figure 5. Macrophages are present in the adrenal medulla throughout post-natal development. A-D. Examples of adrenal cryosections showing that F4/80-ir macrophages (arrow heads) are present throughout the adrenal cortex and medulla (TH-ir zone) in male mice at postnatal days 1 to 50. E, F. F4/80-ir macrophages in the cortex and medulla of female mice. G. Group data showing the relative density of F4/80-ir cells in the adrenal medulla at P25 and P50 (mean # / 0.01 mm^2 ± SD, n = 3 - 4 mice). Scale bar 100 µm.

Figure 6. Adrenal macrophages express P2Y purinergic receptors. A. Adrenal cryosections from a Lyz2cre-GCaMP6f-tdTomato mouse, co-stained for RFP and F4/80 (upper panel) and RFP and CD45 (lower panel). Quantification of immunoreactivity within the medulla (n = 3 mice, 67 – 171 cells per mouse), shows that RFP-ir co-localizes with F4/80- and CD45-ir (R+/F+ and R+/C+, respectively). Most F4/80- and CD-45-ir also co-localizes with RFP-ir (F+/R+ and C+/R+, respectively). B. Example of GCaMP6f fluorescent signal in medulla macrophages in a single adrenal slice from a Lyz2cre-GCaMP6f-tdTomato mouse (left panel, IU = intensity units). Application of 100 µM UDP-Glucose, UDP and UTP is indicated by the green bars. Group data (right panel) showing the response to a panel of P2Y agonists (each applied at 100 µM, mean ± SEM, n = 4 – 10 mice, each open symbol is the average of 15 cells per mouse). C. Calcium increase in response to 100 µM UDP is blocked following application of 100 µM reactive blue-2 (left panel). Group data (right panel; mean ± SEM, n = 4 mice, 15 cells per mouse). * P < 0.05, ** P < 0.01, *** P < 0.001. Scale bar 100 µm. See also Extended Data Figures 6-1 and 6-2 for more details.

Figure 7. Multiple GPCR agonists increase calcium levels in adrenal macrophages. A. Examples of GCaMP6f fluorescence changes in medulla macrophages in response to 100 µM ACh, 100 µM histamine, 100 µM norepinephrine and 1 µM bradykinin (left panel). Group data quantifying the change in GCaMP6f signal in response to multiple agonists (right panel; mean ± SEM, n = 3 - 9 mice, 15 cells per mouse, 100 µM ACh, norepinephrine, oxotremorine-M, histamine; 50 µM DMPP; 10 µM LPA; 1 µM NPY, substance P, angiotensin II, bradykinin, PACAP, met-enkephalin). B. GCaMP6f fluorescence signal in macrophages in an adrenal slice in response to histamine application (left panel). Group data (right panel; mean ± SEM, n = 3 - 5 mice, 15 cells per mouse; EC_{50} ~ 2.7 µM). C. Calcium increase in medulla macrophages in response to 10 µM histamine is blocked by 0.1 µM pyrilimine maleate (H1 receptor antagonist), but not by 10 µM cimetidine (H2 receptor antagonist). Left panel; each trace is the average of 15 cells in a single adrenal slice). Group data quantifying the effect (right panel; mean ± SEM, n = 3 - 4 mice, 15 cells per mouse). D. Sample records showing the response to 100 µM histamine is reduced in the absence of external calcium (left panel, 15 cells in a single adrenal slice, red and blue arrows indicate the rapid and slow phases of the histamine-evoked increase in GCaMP6f signal). Group data quantifying the histamine-evoked increase in GCaMP6f signal (right panel; mean ± SEM, n = 5 mice, 15 cells per mouse). * P < 0.05, ** P < 0.01 See also Extended Data Figure 7-1 for more details.

Figure 8. Isolation of adrenal macrophages alters the calcium increase in response to GPCR agonists. A. Quantification of the change in GCaMP6f signal in adrenal macrophages *in vitro*, in response to 100 µM histamine, ACh, UDP and ATP. In contrast to the response in

slices, isolated macrophages do not respond to histamine and ACh. B. Lung macrophages in slices and C. peritoneal macrophages *in vitro*, respond to UDP and ATP but not to histamine or ACh. Upper images in A-C show corresponding phase contrast images and RFP fluorescence, respectively. Mean ± SEM, n = 3 - 5 mice, 15 cells per mouse. Scale bar 50 µm.

Fig 1

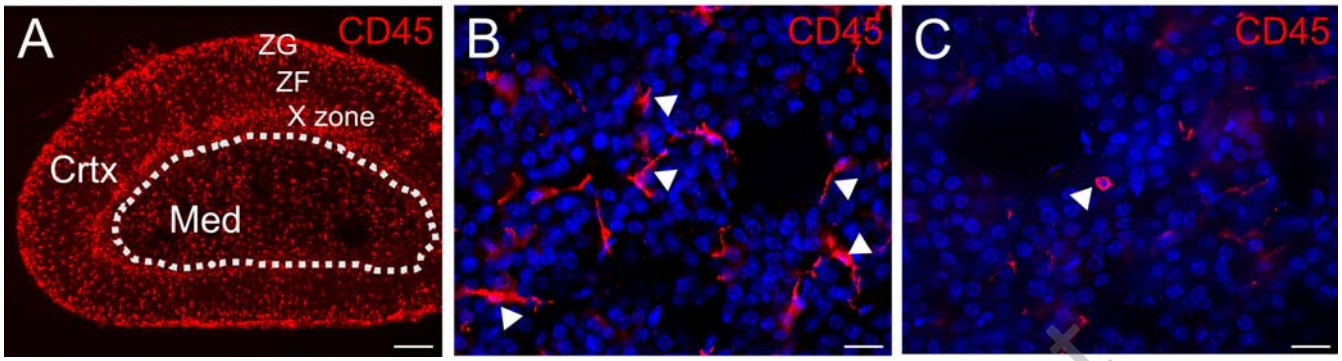

Fig 2

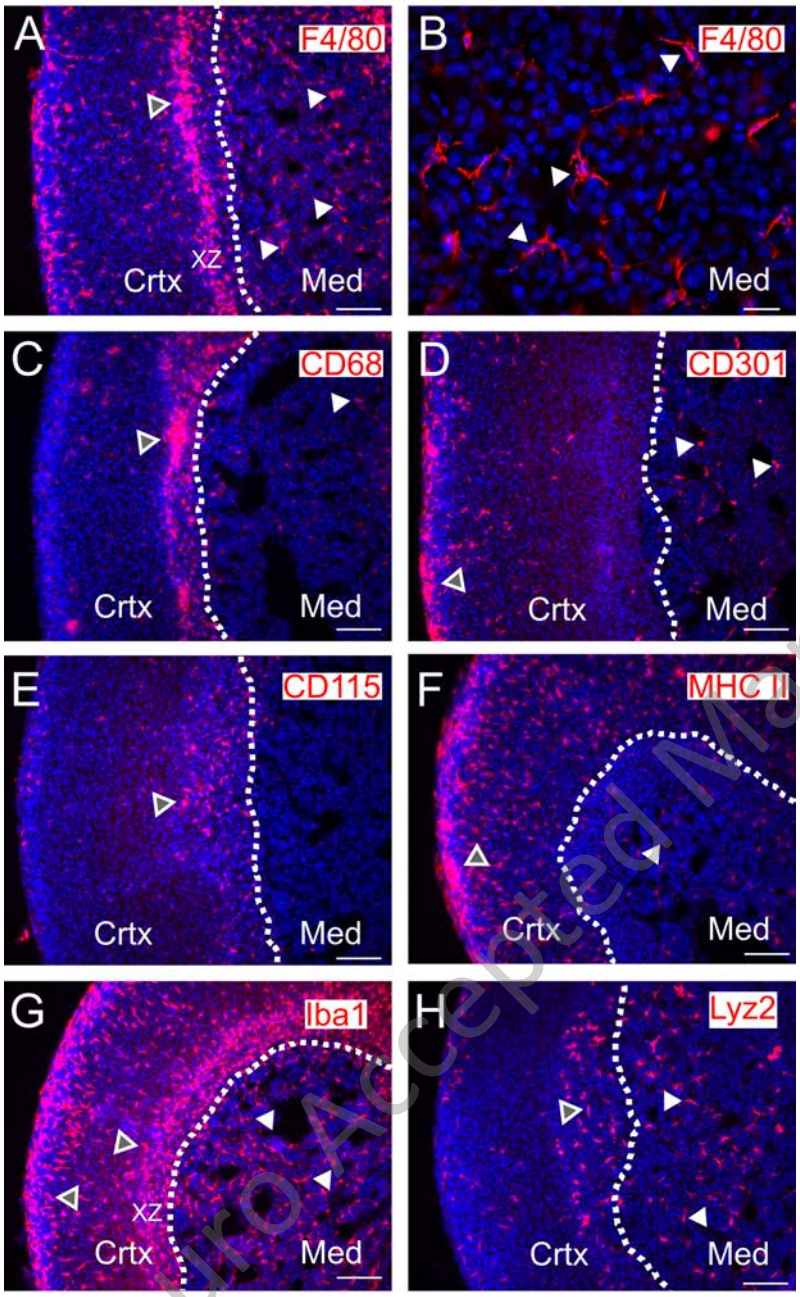

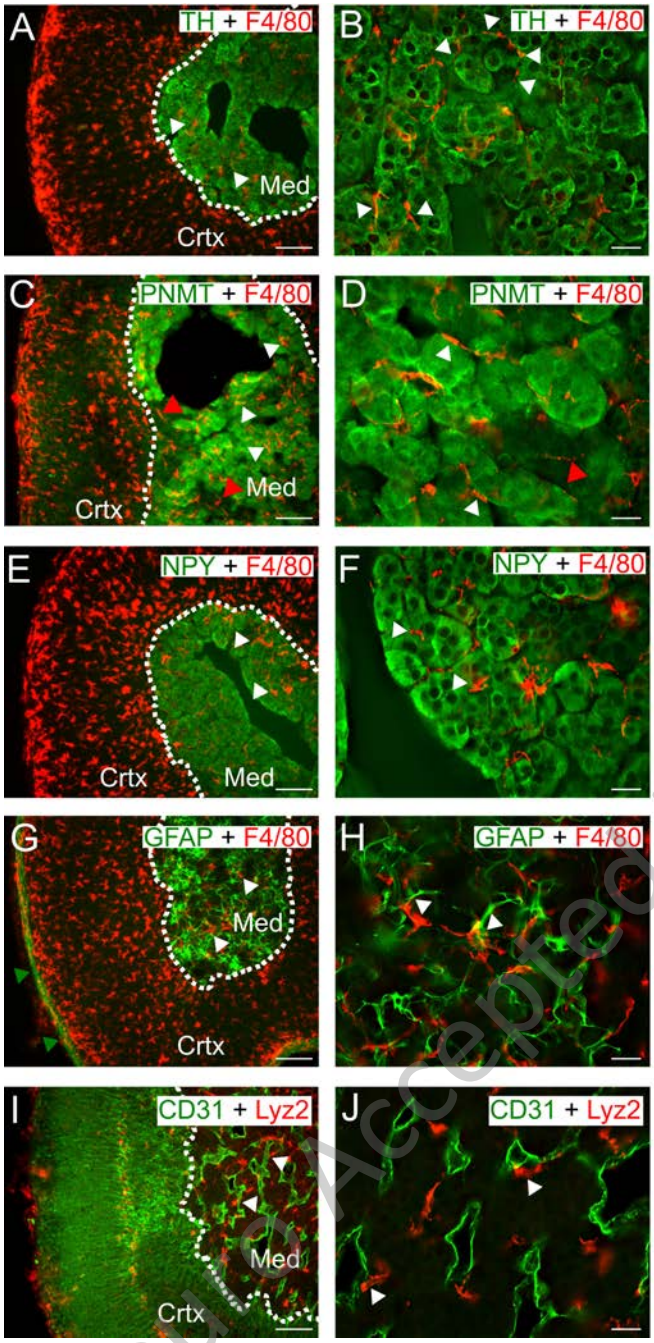

Fig 3

Fig 4

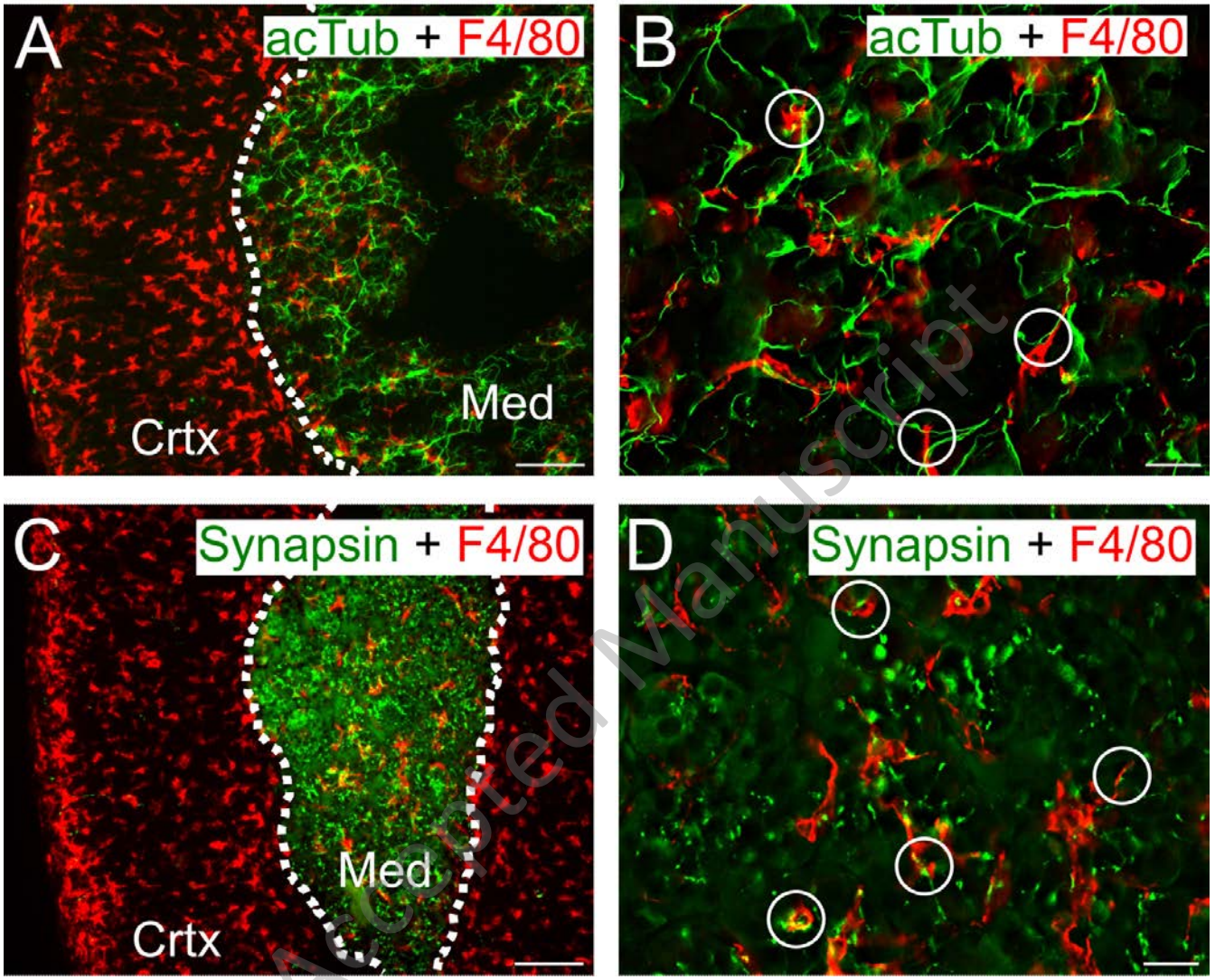

Fig 5

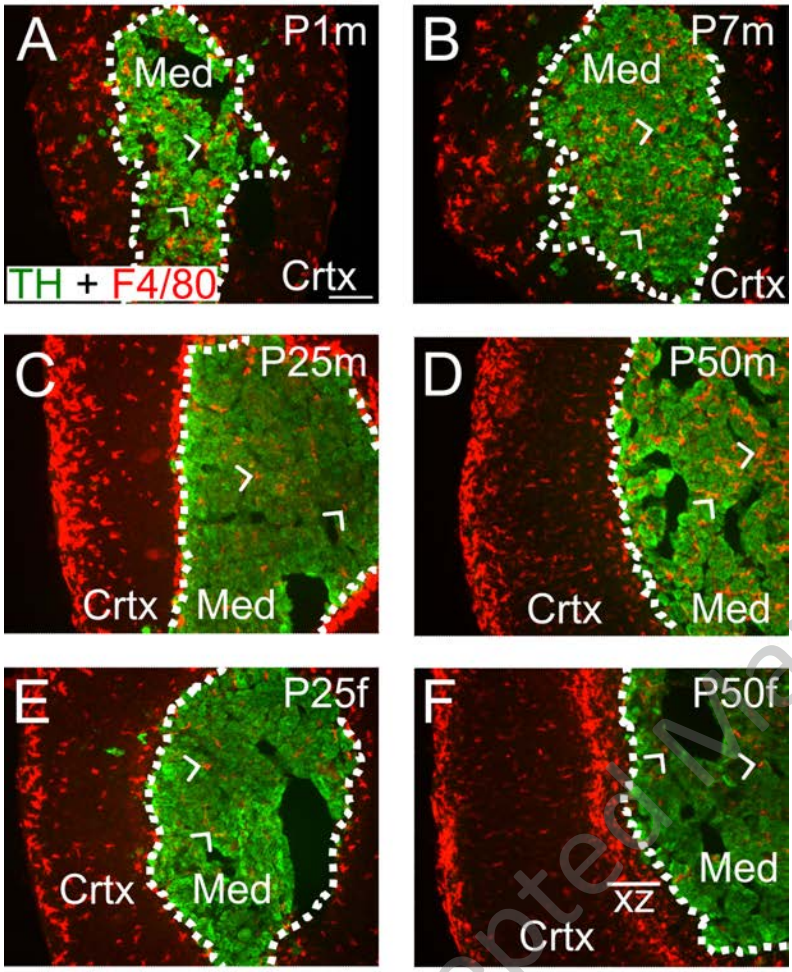

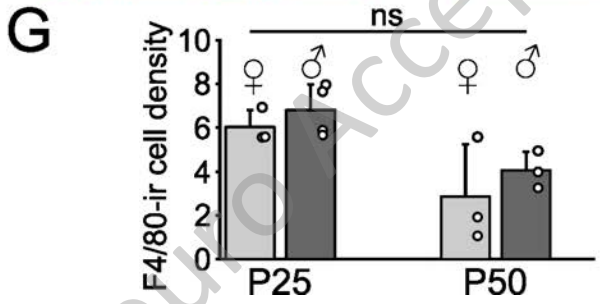

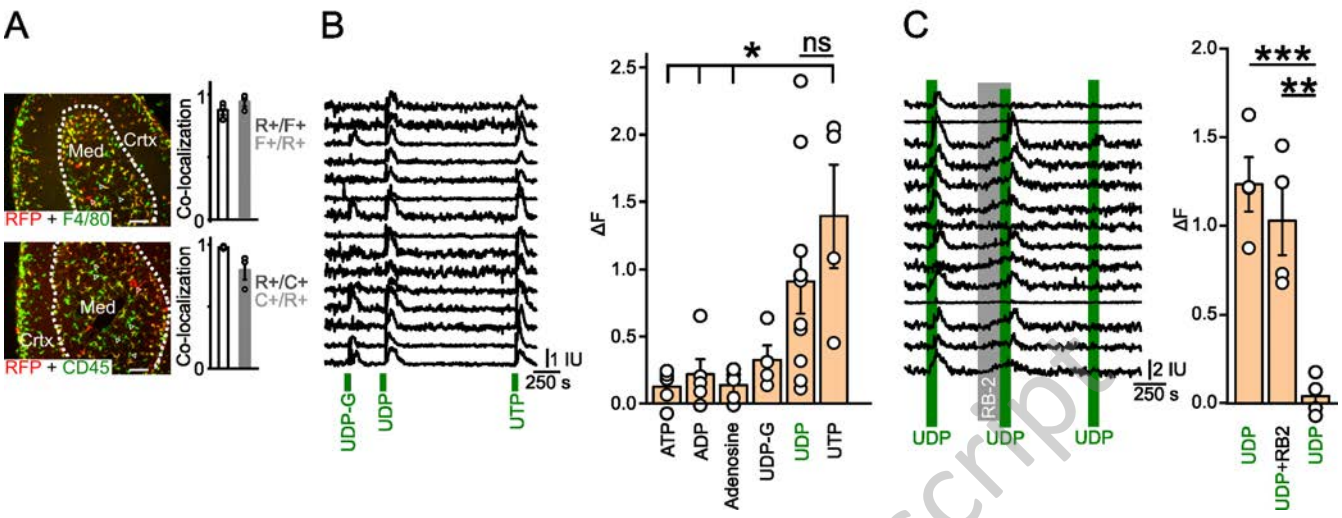

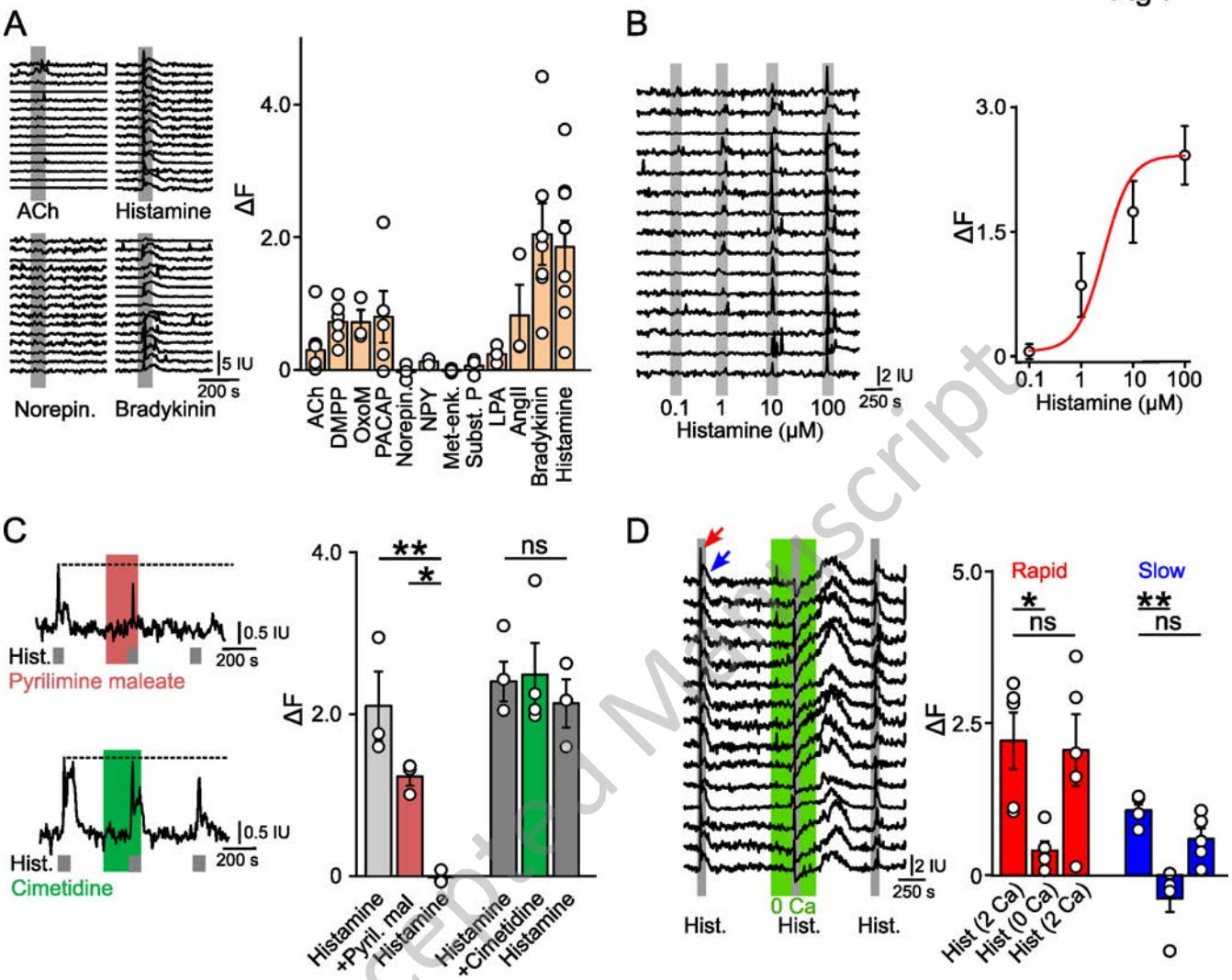

Fig 8